

## Semiconductor-metal transition of the single-domain K/Si(100)-(2 × 1) interface by Fermi-surface determination

J. A. Martín-Gago and M. C. Asensio

*Instituto de Ciencia de Materiales de Madrid-CSIC, Campus de Cantoblanco, 28049 Madrid, Spain*

P. Aebi, R. Fasel, and D. Naumović

*Institut de Physique, Université de Fribourg, CH-1700 Fribourg, Switzerland*

J. Osterwalder

*Physik-Institut, Universität Zürich-Irchel, 8057 Zürich, Switzerland*

M. C. Refolio, J. M. López-Sancho, and J. Rubio

*Instituto de Matemática y Física Fundamental-CSIC, c/Serrano 113, 28006 Madrid, Spain*

The semiconductor-metal electronic transition of the K/Si(100)-(2 × 1) interface is studied by exploring the Fermi surface with photoemission spectroscopy. Once metallized at a critical coverage the surface remains metallic up to saturation. The experimentally determined Fermi surface consists of hole pockets centered around the  $\bar{\Gamma}$  points of the surface Brillouin zone. These results are fairly well reproduced by calculations based on a 2D Mott-Hubbard model. The metallization process is related to the overlap of Si-confined electron clouds surrounding the K atoms rather than to changes in the surface atomic structure.

### I. INTRODUCTION

The adsorption of alkali metals on semiconductor surfaces has been widely studied due to both the technological applications and, the fundamental interest of these interfaces.<sup>1</sup> In particular, the adsorption of alkali-metal overlayer surfaces has suggested the possibility of producing conducting one dimensional chains on top of the Si(100) surface. However, despite the large amount of work devoted to this topic, no agreement has been achieved yet on the description of the basic electronic and atomic properties of these layers.<sup>1</sup> Most of the experimental surface techniques and theoretical methods have been applied for the characterization of these properties. Thus, studies by x-ray photoelectron diffraction (XPD),<sup>2,3</sup> scanning tunneling microscopy (STM),<sup>4,5</sup> angle-resolved ultraviolet photoemission spectroscopy (ARUPS) and inverse photoemission spectroscopy (IPES),<sup>6-8</sup> surface extended x-ray adsorption fine structure (SEXAFS),<sup>5,9</sup> photoelectron spectroscopy (XPS),<sup>10,11</sup> thermal desorption spectroscopy (TDS),<sup>12</sup> first-principles molecular-dynamics calculations,<sup>13</sup> semiempirical self consistent field Hartree-Fock<sup>14</sup> and *ab initio* total-energy calculations<sup>15</sup> have been carried out on these systems and ended up with different structural models and electronic descriptions.

Mainly two different structural models have been proposed for adsorption of alkali metals on Si(100). In the earliest accepted model a single adsorption site on the Si surface is occupied by the Alkali atoms which are located either on pedestal<sup>16</sup> or cave<sup>5</sup> sites [see Figs. 1, sites *b* and *d*, respectively] forming one-dimensional alkali chains (ODAC's) along the  $\langle 001 \rangle$  surface direction.<sup>16</sup> The metallization of this interface is claimed to take place along the ODAC with a saturation coverage of 0.5 ML.<sup>15</sup> However, several studies have subsequently challenged this model, proposing a non-

metallic character of the interface at K saturation. In those works a two-dimensional double-layer model was preferred, with the alkali atoms forming a complete overlayer where both pedestal and valley positions are occupied [see Fig. 1, sites *b* and *c*, respectively].<sup>16</sup> The interface is then expected to become semiconducting at saturation coverage (1 ML).<sup>17</sup> More recent photoemission studies have found just the opposite situation; i.e., after a semiconductor-metal transition, the interface remains metallic up to saturation coverage.<sup>7,8,11</sup>

The disagreement among different experimental results is mainly caused by both the temperature dependence of the saturation coverage and the rapid oxidation of the adsorbed layer.<sup>9</sup> Moreover, the very low photoemission cross section of the states closest to the Fermi energy ( $E_F$ ) renders a clear description of the metallicity difficult. In addition, Si(100) surfaces present a double-domain (DD) structure that gives rise to the mixing of parallel and perpendicular features to the dimer rows (Fig. 1) in angular resolved experiments making their identification and analysis difficult. As will be shown below, special attention has been paid throughout this work to characterizing and avoiding experimental tendencies that can lead to wrong results.

We shall provide some further light on the electronic structure of the K/Si(100) system. The origin of its metallicity of the interface as well as the role of the charge-transfer processes will be studied by measuring the evolution of the Fermi surface (FS) at two different coverages. This will be supplemented by a mean-field calculation based on a 2D Mott-Hubbard model for a monodomain sample which was able to reproduce the experimental FS.

The presence of a FS in a material is a clear signal of metallicity. This FS is of great importance in understanding the properties of materials and epitaxial layers and is commonly mapped by making use of the de Haas-Van Alphen

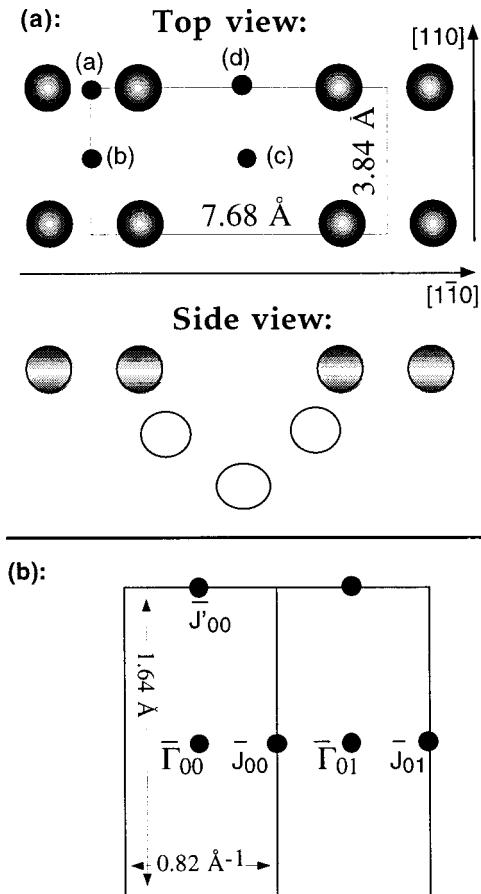


FIG. 1. (a) Schematic representation of the reconstructed Si(100)-(2×1) surface showing the main alkali adsorption sites proposed in the literature: (a) bridge, (b) pedestal, (c) valley, and (d) cave. The 2×1 surface unit cell is represented by a thin line. (b) First and second surface Brillouin zones indicating the main high-symmetry points.

effect. Unfortunately, this technique requires high-purity samples and, in principle, low temperatures, and therefore, it is not suitable for thin layers in ultrahigh vacuum (UHV). Fortunately, ARUPS appeared recently as a powerful tool for measuring the Fermi surface in different compounds, layers, and especially for systems showing electronic phase transitions.<sup>18–22</sup> The FS shape is characteristic of the electronic dimensionality of a system.<sup>21,22</sup> For a three-dimensional (3D) system the Fermi surface measured by ARUPS consists of continuous lines in the  $k$  space corresponding to slices related to the intersection between the 3D Fermi surface and the free-electron final-state sphere.<sup>18</sup> However, for a 2D system, where there is no band dispersion along  $k_{\perp}$ , the Fermi surface can be represented as a prismatic surface in the 3D  $k$  space. Therefore, the Fermi surface of a 2D film is normally characterized by electron and hole pockets around specific points of the surface Brillouin zones (SBZ's).<sup>20,22</sup>

Previous studies on this system by direct and inverse photoemission<sup>8,11</sup> have shown an electron band with parabolic-like dispersion that crosses the Fermi level just above saturation. In a previous paper the presence of a cutoff at the Fermi energy position was reported for coverages above 0.5 ML (Ref. 7) indicating a metallic interface at saturation cov-

erage and nonparabolic dispersion of the electronic states near the Fermi level. In the present work, it will be seen that the K/Si(100)-(2×1) surface has a 2D FS, indicating a well-ordered metallic interface. It will be shown that for lower coverages (approximately one half of the saturation coverage) neither the Fermi edge nor the FS is detected. The 2D Fermi surface is detected at specific points of the SBZ and it consists of hole pockets centered around the  $\bar{\Gamma}$  point of the SBZ. Throughout this article the mechanism responsible for the electronic transition from a semiconducting to a metallic interface will be discussed with the aid of a Mott-Hubbard model for this interface. Specifically, this transition stems from the overlap of the Si electron clouds around the K adsorption sites.

## II. EXPERIMENTAL AND THEORETICAL DETAILS

Experiments were performed with a VG-ESCALAB II spectrometer in an UHV chamber with a base pressure during experiments of  $2 \times 10^{-11}$  mbar. The UHV system is equipped with a motorized two-axis goniometer and with a data acquisition system that allows for fully automatic recording of two-dimensional photoelectron-intensity maps. The overall energy and angular resolution were 35 meV and 1°, respectively. Si(100) crystals were used ( $n$ -type, 30  $\Omega$  cm) for experiments. The angle-resolved UPS measurements were carried out with an unpolarized He lamp ( $h\nu = 21.2$  eV). After several cycles of high-temperature annealing in UHV the typical 2×1 2D surface reconstruction was observed in the LEED pattern. To obtain a SD surface we have evaporated Si on Si(100) following the recipe described in Ref. 23. The LEED pattern corresponding to the clean SD Si(100) surface presented minor, hardly observable spots due to the second domain. K was evaporated from a commercial SAES getter. During evaporation the sample temperature was around 250 K and the pressure never rose above  $10^{-10}$  mbar. The K coverage was estimated by comparing the ratio and evolution of the K and Si 2*p* photoemission peaks with a previously calibrated curve.<sup>9,24</sup> Also, it has been noticed that the XPS intensity of the K 2*p* peak saturates for a particular coverage, i.e., does not increase with evaporation time, as happens in Ref. 9. This coverage will be called the saturation coverage. Experiments have been recorded for two different coverages: Saturation coverage ( $\theta_s$ ), estimated for our experimental setup to be around 0.7 ML in good agreement with previous work<sup>10</sup> and half of the saturation coverage ( $1/2\theta_s$ ), which is around 0.35 ML.

Fermi surface measurements were performed by the method that consists of sequential data acquisition of the total photoemission intensity at the Fermi energy for a complete range of polar and azimuthal emission angles ( $\theta, \varphi$ ). The result is represented as a 2D pattern, where emission angles ( $\theta, \varphi$ ) are transformed in  $k_{\parallel}$  vectors and the photoemission intensity represented as a gray-scale image (Fermi surface map; darker pixels correspond to lower intensities and brighter pixels to higher intensities). An electronic state approaching the Fermi edge will cause a net increase in the total number of emitted photoelectrons at the Fermi energy, and then the intensity maxima in the 3D maps indicate the points of the reciprocal space where a band crosses the Fermi edge. More details about the measurement procedure can be

found in Refs. 18 and 19. The Fermi surface scans presented in this work have been recorded by measuring the number of counts at the Fermi energy with respect to the background for around 3500 angular settings with an angular accuracy of  $1^\circ$ . The surface maps are presented in a linear gray scale. No correction for the instrumental response and no symmetry averaging has been applied to the data.

This interface will be characterized by a 2D Mott-Hubbard model. As shown previously<sup>25</sup> this is a reasonable model as long as one is interested *only* in the electronic structure near the Fermi level. It is then possible to map the results of a full density functional calculation onto an effective 2D Mott-Hubbard model, in such a way that all the information about its geometric structure is somewhere built into the model parameters. This is similar to what happens with many transition-metal oxides.

We therefore adopt an extended Hubbard Hamiltonian with intra-atomic repulsions on the Si atoms (which give rise to the initial semiconducting gap<sup>26</sup>) and interatomic Si-K Coulomb interactions (essentially due to the expected large charge transfers from K to Si). The Si(100) dangling-bond ( $\pi^*$ ) band and the K  $4s$  band are described by including hopping up to next-nearest neighbors, so that both intrachain and interchain interactions are taken into account, thus ensuring the (expected) 2D character of this system. The Si band requires an additional hopping within each dimer. Finally, Si-K hopping is allowed only between nearest neighbors. All these hopping parameters have been scaled to the appropriate distances ( $d$ ) according to the  $1/d^2$  Harrison law<sup>27</sup> (reasonable for  $s$  and  $p$  orbitals). Further, since the Si-K hopping has been calculated by the geometric mean rule, we are left with just two basic hopping parameters (one for Si and another one for K). These can be adjusted directly from standard bulk band-structure calculations<sup>28</sup> so as to reproduce some characteristic feature of Si and K, respectively. The interatomic Si-K Coulomb integral is simply calculated according to the Klopman interpolation formula.<sup>29</sup> The Hubbard repulsion  $U$  on the Si atoms is adjusted to reproduce the experimental gap of the Si(100)-( $2 \times 1$ ) surface, which is known to be about 0.7 eV.<sup>30</sup> This yields  $U \approx 1$  eV. Since all the hopping parameters lie in the interval 0.1–0.3 eV, our system is placed in the weak to moderate coupling regime (the width of the  $\pi^*$  Si dangling-bond band comes out to be  $\approx 0.7$  eV).

This model Hamiltonian will now be treated by the unrestricted Hartree-Fock approximation in its most general version, which includes explicitly transverse ( $S_x$  and  $S_y$ ) spin components in addition to the usual linearization in terms of  $S_z = 0.5 (n_\uparrow - n_\downarrow)$  (longitudinal spin component) and charge  $n = n_\uparrow + n_\downarrow$  (or, what amounts to the same,  $n_\uparrow$  and  $n_\downarrow$ ) of the more conventional Hartree-Fock approximation. The explicit consideration of transverse spin components allows one to deal with both the strong coupling limit (large  $U$ ) where charge fluctuations are absent ( $S_z = 0$ ) and spin fluctuations dominate ( $S_x, S_y \neq 0$ ) and the weak-coupling limit, where charge fluctuations dominate ( $S_x = S_y = 0$  and  $S_z \neq 0$ ). Although the reliability of this approximation has never been really proved, it was used with considerable success in an analysis of possible metal-insulator transitions already in the sixties.<sup>31</sup>

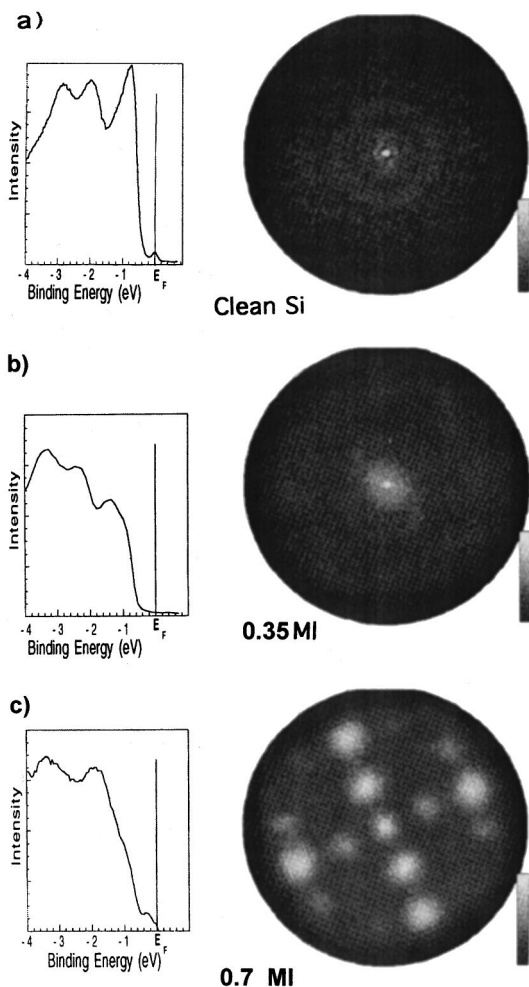


FIG. 2. Valence-band photoemission spectra at normal emission (left) and its corresponding Fermi surface maps (right) for (a) single-domain clean Si(100)-( $2 \times 1$ ) surface, (b) 0.35 ML of K coverage on Si(100), and (c) 0.7 ML of K coverage on Si(100). The photon energy was 21.2 eV.

### III. RESULTS

Several criteria to check the metallicity of an interface can be applied with the photoemission technique. The first consists of detecting the presence of a cutoff in the electronic density at the Fermi energy position. The second is related to the existence of a Fermi surface. The Fermi surface seen by photoemission consists of constant energy contours, which appear as a consequence of the electron bands crossing the Fermi energy at specific points of the reciprocal space. This pattern repeats itself over the different SBZ obtained by shifting the first SBZ through a reciprocal lattice vector of the surface. Therefore the presence of a Fermi surface proves both metallicity and long range order at the interface. Figure 2 shows several valence-band photoemission spectra recorded at normal emission (left hand) together with their respective Fermi surface map (right hand) throughout several SBZ for the clean surface and two different K coverages. At the top left of the figure a spectrum can be seen from the clean SD Si(100)  $2 \times 1$  surface prior to the K deposition. This spectrum shows electronic states at  $-0.8$  eV binding energy, which can be assigned to an occupied surface state associated to the Si dangling bonds.<sup>32</sup> In addition, a little

peak is observed just at the Fermi energy. The presence of this peak is usually attributed to the existence of localized defect states at the Si surface.<sup>33</sup> Coherently with the localized nature of those states, the corresponding Fermi surface map does not show any appreciable dispersion throughout the whole reciprocal space. Upon K deposition for an approximate coverage of around 0.35 ML, a K interface is formed as can be inferred by the absence of emission at the Fermi energy (see Fig. 2, middle-left spectra). The peak associated with surface defects has disappeared. The main electronic state appears now at  $-1.3$  eV instead of  $-0.8$  eV. This is a clear indication of strong interaction between the Si dangling bonds and the arriving K atoms as has been already suggested.<sup>5,32</sup> The corresponding Fermi surface map is presented at the right side of the spectra. The Fermi surface map also indicates the absence of electronic states in other regions of the reciprocal space, supporting a semiconducting character of the interface for this coverage. However, for K coverages around 0.7 ML, i.e., close to saturation coverage, the situation has completely changed. A well-structured peak is present at the Fermi level giving a clear proof of the metallic character of the interface. The corresponding Fermi surface map presents some regions where the photoemission intensity of the K-derived states at the Fermi edge is enhanced.

Figure 3(a) represents the experimentally determined Fermi surface for saturation coverage. The SBZ of the SD Si(100)  $2 \times 1$  reconstruction has been drawn superimposed. It can be appreciated in this figure that the repetition of the feature at the zone center (surface  $\bar{\Gamma}$  point) corresponds of the  $2 \times 1$  reconstruction. Also, little peaks can be appreciated at the  $\bar{J}$  points of the SBZ [see Fig. 1(b)]. These features correspond to the minority second domain and the intensity ratio of the major and minor domains is in agreement with the LEED spot intensities. Thus, it can be concluded that the Fermi surface of this interface is dominated by bands crossing the Fermi edge in a region of the reciprocal space close to the surface  $\bar{\Gamma}$  points. The well-defined Fermi surface repeated through the whole reciprocal lattice makes the two-dimensional character of the metallic band evident, rather than the one-dimensional metallicity predicted by the OADC model.<sup>16</sup> Figure 3(b) represents our calculated Fermi surface for this interface, following the method described in Sec. II. As can be seen, the agreement is fairly good.

In order to understand what kind of electronic features are responsible for the enhancement of intensity around the  $\bar{\Gamma}$  points, valence-band spectra for different emission angles have been measured previously.<sup>7</sup> Their corresponding dispersions as a function of the  $k_{\parallel}$  vector along the  $J$ - $\bar{\Gamma}$ - $J$  direction (perpendicular to the Si dimers rows) of the second SBZ [see Fig. 1(b)] is shown in Fig. 4. Also in this figure, our calculated bands have been drawn on the same graph. Two K-induced bands dispersing downwards from the  $\bar{\Gamma}$  point very close to the Fermi edge are clearly seen. These electronic states will be labeled hereafter  $F1$  and  $F2$ . At normal emission, their corresponding peaks are centered at 0.3 and 0.1 eV from the Fermi energy, respectively. The presence of these states very close to the Fermi energy is responsible for the enhancement of intensity appreciated in the Fermi Surface maps around the  $\bar{\Gamma}$  points.

Due to the natural width of the valence-band states,<sup>20,21</sup> to

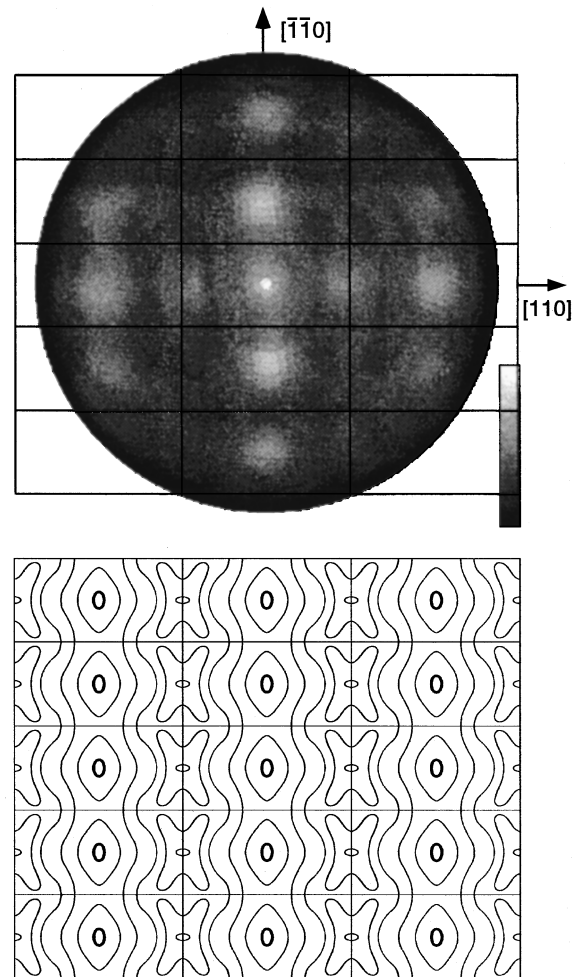


FIG. 3. (Top) Experimental Fermi surface map of the K/Si(100) system at saturation coverage. The surface Brillouin zones have been drawn superimposed. (Bottom) Calculated Fermi surface map with a Mott-Hubbard model.

the experimental energy resolution and to the Fermi edge cutoff, the binding energy of the electronic states close to the Fermi energy cannot be precisely assigned and, therefore, any photoemission peak appearing with binding energy smaller than 0.1 eV will contribute to the measured intensity of the Fermi surface maps.<sup>21</sup> Therefore, it may happen that the  $F1$  state approaches the Fermi energy without crossing it, rendering the surface, in an accurate sense, semiconducting. Thus additional proofs for the metallicity should be given. Riffe *et al.* have shown<sup>10</sup> by XPS that as the coverage increases, a change in the K  $3p$  binding energy together with an enlargement of the singularity index are detected. Similar behavior is found in our case (core-level shift and enlargement of the K  $2p$  peak) clearly indicating a transition from a semiconducting to a metallic surface. Thus, it can be concluded that the features seen in Fig. 3(a) correspond to the Fermi surface created by hole pockets recorded over eleven different SBZ's at saturation coverage of the K/Si(100) system.

One of the reasons for the disagreement existing in the scientific literature about the metallicity of this interface can be due to the rapid contamination of the K layer. In addition to that, the photoemission cross section for  $KO_x$  compounds

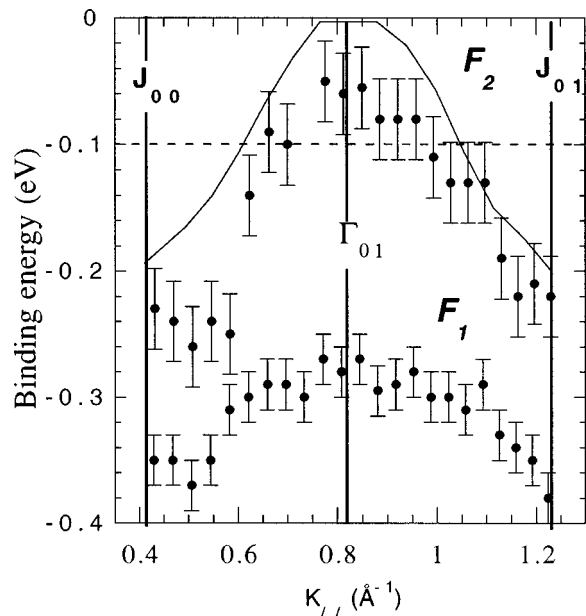


FIG. 4. Surface band dispersion near the Fermi level at saturation coverage along the  $J$ - $\bar{\Gamma}$ - $J$  direction [see Fig. 1(b)]. Points above the straight line at  $E = -0.1$  eV can be considered as belonging to the Fermi surface. The continuous line is the calculated band (see text for details).

in the valence band is very high, causing significant changes in the photoemission spectra. It is important to remark that the emission from the states that cross the Fermi energy around the surface  $\bar{\Gamma}$  point is very sensitive to the residual pressure in the experimental chamber. This point is illustrated in Fig. 5. This figure shows UPS spectra of a K-saturated surface (a), the same spectra 4 h later (b), and again after 10 h (c). Several peaks at the positions marked by arrows (around 6 and 9 eV binding energy) develop with time. These peaks have been found in previous studies of controlled oxidation of the K/Si(100) interface,<sup>34,35</sup> and they are a fingerprint of the presence of oxygen atoms. The total

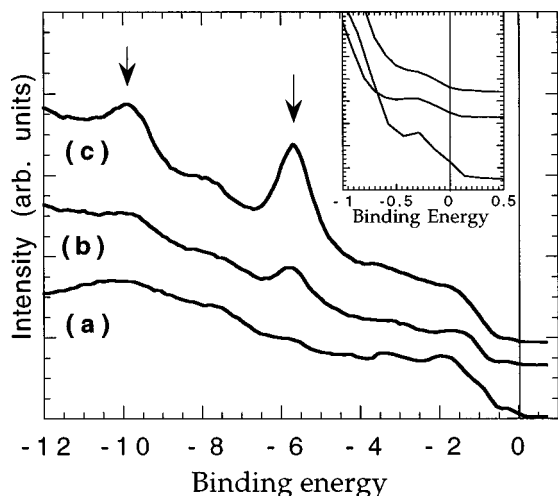


FIG. 5. Curve (a) photoemission spectra of the saturated K/Si(100) surface recorded right after K deposition. (b) Same spectra recorded after 4 h. (c) After 10 h.

amount of oxidation in the case of the spectrum (c) has been estimated by measuring XPS intensities to be around 10%. The effect of the oxidation on the Fermi threshold is shown in the inset of Fig. 5, which corresponds to a zooming of the Fermi energy window. After 4 h working with the sample within the low  $10^{-11}$  mbar range, the emission at the Fermi edge was strongly reduced and after 10 h it was nonexistent. It is important to remark that the base pressure during the experiments reported here was in the low  $10^{-11}$  mbar. If the same experiment is performed at  $10^{-10}$  mbar, a Fermi edge will not be detected on the surface and it is then easily concluded that the surface is semiconducting.

#### IV. DISCUSSION

The combination of theoretical and experimental results presented in this paper provide a consistent picture of the electronic structure of the K/Si(100)-(2 $\times$ 1) interface. As can be seen in Fig. 3, the Fermi surface of this interface consists of small hole pockets centered around the  $\bar{\Gamma}$  points. In most of the recent published work it is concluded that the surface is metallic. Nevertheless, in the present work, the  $F2$  band of Fig. 4 shows a downward dispersion instead of the recently reported upward dispersion.<sup>11,36</sup> The presence of an electron pocket around  $\bar{\Gamma}$  would suggest a quasi-free-electron metallic band and, consequently, a metallization starting within the K overlayer. However, a hole pocket is experimentally found and, therefore, the bands forming the hole pockets must have their origin in the Si substrate. Both interpretations could match with a combined photoemission and inverse photoemission study<sup>8</sup> where, in addition to the occupied states, an unoccupied band ( $U2$ ) is seen at around 0.35 eV above  $E_F$  at the  $\bar{\Gamma}$  point. This band ( $U2$ ) has a paraboliclike dispersion showing a quasi-free-electron-like behavior, as could be derived from K- $4p_z$  electrons. In that work two peaks are seen at each side of the Fermi level (above and below simultaneously). Due to the small energy difference between them (around 0.5 eV) they are usually interpreted as being the same state. However, another possible interpretation of the same data could be that they actually correspond to different states ( $U2$  and  $F2$ ), in agreement with the calculation of Ref. 13. Thus, in Ref. 11 it is claimed that the  $F2$  band is due to a partial occupation of a K- $sp_z$  band ( $S3$  of Ref. 13) based on the symmetry and upward dispersion of this state.<sup>8,11,13,32</sup> However, this argument can be discarded on the basis of a simple electron counting argument: If one electron per K atom is assumed, there would be two electrons per Si dimer, and then not enough electrons would be available to fill the  $S1$  and  $S2$  bands (see Ref. 13). Therefore, we rather believe that the unoccupied band of Ref. 8 is remaining above  $E_F$  at the  $\bar{\Gamma}$  point.

The good agreement between theory and experiment as seen in Figs. 3 and 4 suggests that the scenario of our experimental interpretation and calculation should be accurate. It was carried out assuming a full monolayer of K atoms and admitting a small fraction of its electrons to go into trapping centers, so that the Si  $\pi^*$  antibonding band does not get completely filled. This assumption is equivalent to supposing that the saturation coverage does not correspond to 1 ML. If it did, we would inevitably have a semiconducting interface.

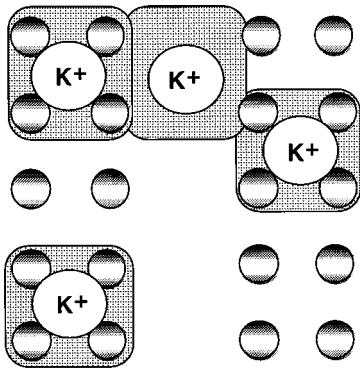


FIG. 6. Schematic representation of the metallization process. The shadowed area represents the spatial region where the total Si charge distribution around a K atom is larger than unity.

Thus, the  $\pi^*$  band, initially empty for the Si surface, receives almost two electrons per dimer with its maximum (at the  $\bar{\Gamma}$  point) left empty (hole pocket). On the other hand, our experimental bands are in close agreement with the band structure near the Fermi level found by Kobayasi *et al.*<sup>13</sup>

The existence of a Fermi surface repeated with the periodicity of the surface over 11 different SBZ consisting of hole pockets for saturation coverage excludes K clustering. Several authors have explained the existence of a density of states at the Fermi energy<sup>37</sup> as related to an excess of K atoms, forming clumps on the surface, which would lead to a metallic Fermi threshold without long-range order. Existence of ordered K clusters can also be ruled out due to the absence of anisotropy in the photoelectron diffraction azimuthal scans for polar angles lower than  $72^\circ$  (data not shown). Therefore, Fig. 3(a) suggests a two dimensional model with K atoms adsorbed in hollow and valley sites as has been suggested by XPD experiments.<sup>2</sup>

In Fig. 2 it is shown that the rise of the Fermi surface is directly related to a critical coverage. A possible interpretation for such an electronic transition can be found in terms of charge localization. Indeed although the K atoms transfer charge to the Si dangling-bond states, the transferred electrons are not initially free to move around the surface, but instead remain localized around the K sites. Figure 6 which shows schematically the spatial region with total charge distribution larger than unity on the Si atoms surrounding a  $K^+$  ion is (more details about this calculation can be found in Ref. 38). From a critical coverage onwards, therefore, this electron clouds will collapse, the spatially localized electrons being then transferred to the bands. Notice, however, that the  $K^+$  ions must feel a strong coulomb repulsion, which tends to work against their excessive accumulation on top of the Si surface. Since the K-K distance in a bcc bulk crystal is 4.53 Å, considerably larger than the corresponding distance on the Si(100) surface, 3.84 Å (Fig. 1), the K atoms will repel strongly near saturation coverage. This repulsion could be the driving force limiting the K coverage on the surface. Thus, differences in both the critical and the saturation coverage are to be expected when other alkali metals are adsorbed on Si(100) surfaces. Recently the metallicity of Li-covered Si surfaces has been reported at 0.25 ML.<sup>39</sup>

From the above explanation, one is tempted to believe that adsorption takes place first at hollow sites, as predicted by the ODAC model,<sup>16</sup> and then, when most of these sites

are completed, at valley positions. This would lead to a semiconducting interface at full saturation coverage, i.e., if the second layer were fully completed. However, our experimental and theoretical results indicate that once the transition of the interface from semiconducting to metallic takes place with increasing coverage, the interface remains metallic all the way up to saturation. No reentrant semiconducting behavior is ever found in this coverage range, probably indicating that the second layer is not fully occupied. The 2D symmetry of the interface right after metallization notice above does not support previous models suggesting 1D behavior. This is the case of the ODAC model where metallization at low coverages is induced by a unique adsorption site along the Si dimer chains. To gather further evidence, we have performed photoelectron diffraction azimuthal scans for low and high-K coverages, a technique that samples short-range order at the surface. The same features in azimuthal scans were obtained in the two cases, indicating that both sites were occupied indistinctly from the beginning of the growth (data not shown). Therefore the semiconducting-metallic transition does not seem to be a structural transition, but must be rather electronic in nature. As shown in Fig. 2, the metallization is induced by K electrons which start to fill the  $\pi^*$  band of Si. This transition takes place at a critical coverage.

The disappearance of the Fermi edge upon oxidation of the surface shown in Fig. 5 suggests that electrons are trapped by approaching O atoms (or other electronegative species from the residual gas), thus preventing charge transfer to the Si dangling bonds. Therefore, the Si electron clouds discussed above will be spatially separated and then the metallization process disrupted. As a consequence, a transition in opposite sense to that described in Fig. 2 (i.e., from a metallic to a semiconducting interface) will be observed by the photoemission technique.

## V. CONCLUSIONS

In summary, we have studied the adsorption of K atoms on the SD Si(100)-(2×1) surface. Our results show that there is a critical coverage for which a semiconductor-to-metal transition takes place, as experimentally evidenced by the existence of a bidimensional Fermi surface for saturation coverage. This FS consist of hole pockets centered around the  $\bar{\Gamma}$  points of the SBZ. These experimental observations are confirmed by a mean-field calculation based on a Mott-Hubbard model where the K atoms (partially ionized) transfer electron charge to the antibonding  $\pi^*$  orbital. This transition does not seem related to structural changes at the surface but rather to the overlap of Si-confined electron clouds around the K atoms.

## ACKNOWLEDGMENTS

This work was partially funded by the Spanish agency DGICYT under Grant No. PB94-0022-c02-01 and PB92-0030 and by the support of the Large Scale Installation Program of the E.C. assigned to LURE. Skillful technical assistance was provided by E. Mooser, O. Raezo, O. Zosso, F. Bourqui, and Ch. Neururer. This project has been supported by the Fonds National Suisse pour la Recherche Scientifique.

- <sup>1</sup>Several reviews can be found in *Metallization and Metal-Semiconductor Interfaces*, Vol. 195 of *NATO Advanced Study Institute, Series B: Physics*, edited by I. P. Batra (Plenum, New York, 1989).
- <sup>2</sup>Y. Enta, T. Kinoshita, S. Suzuki, and S. Kono, *Phys. Rev. B* **36**, 9801 (1987).
- <sup>3</sup>J. Osterwalder, P. Aebi, R. Fasel, D. Naumović, P. Schwaller, T. Kreuz, L. Schlapbach, T. Abukawa, and S. Kono, *Surf. Sci.* **331**, 1002 (1995).
- <sup>4</sup>U. A. Effner, D. Batz, J. Binder, T. Bertrams, A. Brodde, Ch. Lunau, H. Nedermeier, and M. Hanbcken, *Surf. Sci.* **277**, 207 (1992).
- <sup>5</sup>P. Soukiassian, J. A. Kubbi, P. S. Mangat, Z. Hurych, and K. M. Schirm, *Phys. Rev. B* **46**, 13 471 (1992).
- <sup>6</sup>Abukama *et al.*, *Surf. Sci.* **261**, 217 (1992).
- <sup>7</sup>J. A. Martín-Gago, M. C. Asensio, F. Soria, P. Aebi, R. Fasel, D. Naumović, and J. Osterwalder, *Surf. Sci.* **307**, 995 (1994).
- <sup>8</sup>L. S. O. Johansson and B. Reihl, *Phys. Rev. Lett.* **67**, 2191 (1991).
- <sup>9</sup>L. Spies, P. S. Mangat, S.-P. Tang, K. M. Schirm, A. J. Freeman, and P. Soukiassian, *Surf. Sci. Lett.* **289**, L631 (1993).
- <sup>10</sup>D. M. Riffle, G. K. Wertheim, J. E. Rowe, and P. H. Citrin, *Phys. Rev. B* **45**, 3532 (1992).
- <sup>11</sup>P. Segovia, G. R. Castro, A. Mascaraque, P. Prieto, H. J. Kim, and E. G. Michel, *Phys. Rev. B* **54**, 14 277 (1996).
- <sup>12</sup>E. G. Michel, P. Pervan, G. R. Castro, R. Miranda, and K. Wandelt, *Phys. Rev. B* **45**, 11 811 (1992).
- <sup>13</sup>K. Kobayashi, Y. Morikawa, K. Terakura, and S. Blugel, *Phys. Rev. B* **45**, 3469 (1992).
- <sup>14</sup>R. Ramirez, *Phys. Rev. B* **40**, 3962 (1989).
- <sup>15</sup>I. P. Batra, E. Tekman, and S. Ciraci, *Prog. Surf. Sci.* **36**, 289 (1991).
- <sup>16</sup>J. D. Levine, *Surf. Sci.* **34**, 90 (1973).
- <sup>17</sup>In this work 1 ML coverage corresponds to the number of atoms which form the  $(1 \times 1)$ -Si(100) surface.
- <sup>18</sup>P. Aebi, J. Osterwalder, R. Fasel, D. Naumović, and L. Schlapbach, *Surf. Sci.* **307**, 917 (1994).
- <sup>19</sup>P. Aebi, J. Osterwalder, P. Schwaller, L. Schlapbach, M. Shimoda, T. Mochiku, and K. Kadowaki, *Phys. Rev. Lett.* **72**, 2757 (1991).
- <sup>20</sup>K. E. Smith and S. D. Kevan, *Phys. Rev. B* **43**, 3986 (1991).
- <sup>21</sup>K. E. Smith, K. Breuer, M. Greenblat, and W. McCarroll, *Phys. Rev. Lett.* **70**, 3772 (1993).
- <sup>22</sup>J. A. Martín-Gago, J. Y. Veuillen, C. Casado, and M. T. Nguyen, *Phys. Rev. B* **55**, 5129 (1997); P. Wetzel, C. Pirri, P. Paki, L. C. Peruchetti, D. Bolmont, and G. Gewinner, *Solid State Commun.* **82**, 235 (1992).
- <sup>23</sup>Y. Sasaki, Y. Enta, S. Suzuki, and S. Kono, *Surf. Sci.* **276**, 205 (1992).
- <sup>24</sup>E. M. Oellig, E. G. Michel, M. C. Asensio, R. Miranda, J. C. Durán, A. Muñoz, and F. Flores, *Europhys. Lett.* **5**, 727 (1988).
- <sup>25</sup>M. C. Refolio, J. M. López Sancho, M. P. López Sancho, and J. Rubio, *Phys. Rev. B* **53**, 4791 (1996).
- <sup>26</sup>J. M. López Sancho, M. C. Refolio, M. P. López Sancho, and J. Rubio, *Surf. Sci.* **285**, L491 (1993); *J. Vac. Sci. Technol. A* **11**, 2483 (1993).
- <sup>27</sup>W. A. Harrison, *electronic structure and properties of solids* (Freeman, San Francisco, 1980).
- <sup>28</sup>D. A. Papaconstantopoulos, *Handbook of the Band Structure of Elemental Solids* (Plenum, New York, 1996).
- <sup>29</sup>G. Klopman, *J. Am. Chem. Soc.* **86**, 4550 (1964).
- <sup>30</sup>R. I. G. Uhrberg, G. V. Hansson, J. M. Nichols, and S. A. Flodström, *Phys. Rev. B* **24**, 4684 (1981).
- <sup>31</sup>N. F. Mot, *Philos. Mag.* **20**, 1 (1969).
- <sup>32</sup>Y. Lyng, A. J. Freeman, and B. Delley, *Phys. Rev. B* **39**, 10 144 (1989).
- <sup>33</sup>G. Rossi, *Surf. Sci. Rep.* **7**, 1 (1987).
- <sup>34</sup>G. R. Castro, P. Pervan, E. G. Michel, R. Miranda, and W. Wandelt, *Vacuum* **41**, 787 (1990).
- <sup>35</sup>M. C. Refolio, J. M. López Sancho, M. P. López Sancho, and J. Rubio, *Phys. Rev. B* **49**, 2629 (1994).
- <sup>36</sup>P. Segovia, G. R. Castro, A. Mascaraque, and E. G. Michel, *Surf. Sci.* **377**, 220 (1997).
- <sup>37</sup>T. Abukawa and S. Kono, *Phys. Rev. B* **36**, 9801 (1987) and references therein.
- <sup>38</sup>M. C. Refolio, J. Rubio, M. P. López Sancho, and J. M. López Sancho, *Phys. Rev. B* **49**, 4623 (1994).
- <sup>39</sup>K. D. Lee, C. Y. Kim, and J. W. Chung, *Surf. Sci.* **366**, L709 (1996).